MOLECULAR PHARMACOLOGY, 15, 545–558

Characterization of Muscarinic Acetylcholine Receptors from Mouse Brain: Evidence for Regional Heterogeneity and Isomerization

YOEL KLOOG, YAACOV EGOZI AND MORDECHAI SOKOLOVSKY

The George S. Wise Faculty of Life Sciences, Department of Biochemistry, Tel-Aviv University, Tel-Aviv, Israel

(Received August 17, 1978)
(Accepted November 17, 1978)

SUMMARY

KLOOG, YOEL, EGOZI, Y. & SOKOLOVSKY, M. (1979). Characterization of muscarinic acetylcholine receptors from mouse brain. Evidence for regional heterogeneity and isomerization. *Mol. Pharmacol.*, **15**, 545–558.

High affinity binding of tritium labeled N-methyl-4-piperidyl benzilate to homogenates from various regions of mouse brain is used to characterize the binding mechanism to specific muscarinic sites at 25°. Binding experiments at equilibrium reveal differences in the affinity of various muscarinic agonists and antagonists for the binding sites in the various regions: cortex, putamen, hippocampus, medulla pons, and cerebellum. The density of muscarinic binding sites is also different in these regions. The regional heterogeneity is further investigated by kinetic experiments which measure the rates and the mechanisms of association and dissociation of [^{3}H]-N-methyl-4-piperidyl benzilate. These experiments suggest that while each region contains a homogeneous population of binding sites, the association and dissociation of the ligands do not follow a simple first order mechanism. The simplest model which fits the experimental findings and which is compatible with previously published models, consists of a fast binding step followed by a slow isomerization process of the receptor-ligand complex.

INTRODUCTION

The binding to muscarinic receptors prepared from whole mouse brain was recently examined using the potent and highly specific antagonists 4-NMPB,[1] scopolamine and atropine which were radiolabeled to a high specific activity (1–3). The binding assay with these antagonists, based on the filtration technique, enabled us to investigate directly the ligand specificity in conjunction with detailed kinetic studies. From previous studies it was concluded that binding of antagonists to the muscarinic receptors proceeds by a two-step mechanism: a fast binding step followed by a slow isomerization process of the receptor-ligand complex (1–3). A two-step mechanism was recently described also for the muscarinic receptors in developing chick heart (4), retina (5) and in the iris of albino rabbit (6) and cat (7).

The kinetic experiments carried out previously with the whole mouse brain preparation favored the assumption that antagonists bind to a homogeneous population of binding sites (1–3). However, heterogeneity of receptors could not be dismissed altogether. Hence, the purpose of the present work was to investigate the characteristics of the regional distribution of *in vitro* binding of [^{3}H]-4NMPB and [^{3}H]-atropine in mouse brain. Kinetic as well as equilibrium analysis of the binding in different brain regions were used to probe the nature of

[1] The abbreviations used are: 4-NMPB, N-methyl-4-piperidyl benzilate; [^{3}H]-4NMPB, [^{3}H]-N-methyl-4-piperidyl benzilate; QNB, quinuclidinyl benzilate.

0026-895X/79/030545-14$02.00/0

the binding sites and the possible differences between specific muscarinic sites in the various regions. An analysis of association and dissociation parameters for the interaction of [^{3}H]-4NMPB with muscarinic binding sites was performed in order to characterize the dynamic steps involved in the interaction of the labeled drug with the receptors. A preliminary report of some of these studies has been published (8).

MATERIALS AND METHODS

Materials. [^{3}H]-atropine 2.6 Ci/mmole, and [^{3}H]-4NMPB 6 Ci/mmole were prepared by catalytic tritium exchange as described elsewhere (2). The chemical and radiochemical purity was determined by analytical thin-layer chromatography (Merck Silica 60 plates, 0.25 mm thickness) in two solvent systems: n-butanol, acetic acid, water (4:1:1), and chloroform, acetone, diethylamine (5:4:1). [^{3}H] labeled drugs moved as a single peak, identical to the authentic unlabeled compound in these two systems. The purity was >99% for [^{3}H]-atropine and >97% for [^{3}H]-4NMPB.

(+) QNB and (−) QNB were prepared as described elsewhere (9). Other compounds were: oxotremorine (Aldrich), scopolamine HBr (Plantex, Israel), atropine sulfate hydrate, acetylcholine, carbamylcholine chloride, propranolol and d-tubocurarine (Sigma); all other compounds were of the best grade available.

Methods. Male ICR mice (20–25 g) were decapitated, brains were rapidly removed and the brain areas were dissected in a cold room after identification with the aid of the *Stereotaxic Atlas of the Albino Mouse Forebrain* (10). After dissection, brain regions (from 15–25 mice for the caudate putamen, 10–15 mice for the hippocampus, and 5–10 mice for other regions) were homogenized in ice cold 0.32 M sucrose using a motor-driven teflon pestle (950 rpm) in a glass homogenizer to yield a 10% homogenate (W/V). In order to achieve a constant receptor density the preparations were further diluted whenever necessary in 0.32 M sucrose to obtain a desired protein content. Unless otherwise indicated 50 μl of tissue preparation were incubated as described previously (2, 3) at 25°, in 2 ml modified Krebs-Hensleit solution (25 mM Tris-HCl, 118 mM NaCl, 4.69 mM KCl, 1.9 mM $CaCl_2$, 0.54 mM $MgCl_2$, 1.0 mM NaH_2PO_4, 11.1 mM glucose), pH 7.4, containing the labeled ligand. After various incubation times, ice cold Krebs solution (3 ml) was added and the contents were passed rapidly through a glass filter (GF/C, Whatman 25 mm diameter) by suction. The filters were washed 3 times (3 ml of ice cold Krebs solution). All procedures were completed within less than 10 sec and all binding experiments were performed in triplicate together with triplicate samples containing 5×10^{-5} M of unlabeled ligand. The filters were placed in vials containing 5 ml of scintillation liquid (330 ml Triton-X-100, 660 ml toluene, 5.5 g PPO (Packard) and 0.1 g dimethyl-POPOP (Merck)) maintained at 25° for 30 min and the radioactivity then assayed by liquid scintillation spectrometry (Packard Prias model PL). Standard tritiated water (Packard) was used to establish the efficiency of counting 40–45%. Protein was determined by the method of Lowry *et al.* (11) using bovine serum albumin as a standard.

Specific binding is defined as the total minus the nonspecific binding, i.e., binding in the presence of 5×10^{-5} M of unlabeled 4-NMPB and atropine.

The total binding in the S_1 (1000 × *g*, 10 min supernatant) and P_2 (17,500 × *g*, 20 min pellet resuspended) fractions was similar and represented 85% of the binding in the whole tissue homogenate. The total binding in fractions P_1 (1000 × *g*, 10 min pellet resuspended) and S_2 (17,500 × *g*, 20 min supernatant), on the other hand, was relatively low. In the presence of excess (5 μM) unlabeled 4-NMPB or atropine, the total binding of the whole brain homogenate and of fractions S_1 and P_2 was reduced to less than 10% of the values recorded in the absence of unlabeled drug. No change was found, under the same conditions, in the total binding of fractions P_1 and S_2. Consequently the experiments were carried out with the whole tissue homogenate.

Possible chemical alterations of [^{3}H]-4NMPB and [^{3}H]-atropine in the course of a binding experiment was tested by thin-layer chromatography. After 60 min of incubation aliquots were chromatographed as

described in MATERIALS. [^{3}H]-labeled compounds moved as a single peak with the same R_F as authentic samples.

Competition experiments and the analysis of binding kinetics were carried out as described in details in previous reports (1, 2).

RESULTS

Equilibrium binding. The binding of [^{3}H]-4NMPB and [^{3}H]-atropine at 25° was studied in homogenates of the following brain regions: cortex, caudate putamen, hippocampus, medulla pons, and cerebellum.

The concentration dependence of specific binding of [^{3}H]-4NMPB at equilibrium is shown in Fig. 1 for each of the five separate regions. As reported previously for the binding of this ligand to whole brain homogenate (2), the specific binding is shown in Fig. 1 to be saturable in the concentration range of 0.25–10 nM [^{3}H]-4NMPB. The nonspecific binding (not shown) represented 8–10% of total binding even at the highest ligand concentration used, in all brain regions except in the cerebellum where the receptor density is much lower (see below) and where the non-specific binding was relatively higher. Even these higher values did not, however, interfere with the reliable determination of binding parameters. Similar results were obtained with [^{3}H]-atropine as ligand.

The specific binding of [^{3}H]-4NMPB was found to be linear as a function of protein concentration in each of the five regions, up to 0.8 mg protein per assay. Tissue concentrations of 0.2–0.7 mg protein per assay were therefore used for all experiments. Double reciprocal plots as well as the Scatchard (12) representations of the equilibrium binding data shown in Fig. 2, yielded straight lines for each of the five regions examined, indicating a homogeneous population of high-affinity binding sites within each region, in the concentration range examined.

Table 1 shows the regional distribution of receptors labeled by [^{3}H]-4NMPB and [^{3}H]-atropine in mouse brain. The concentration of high affinity binding sites seems

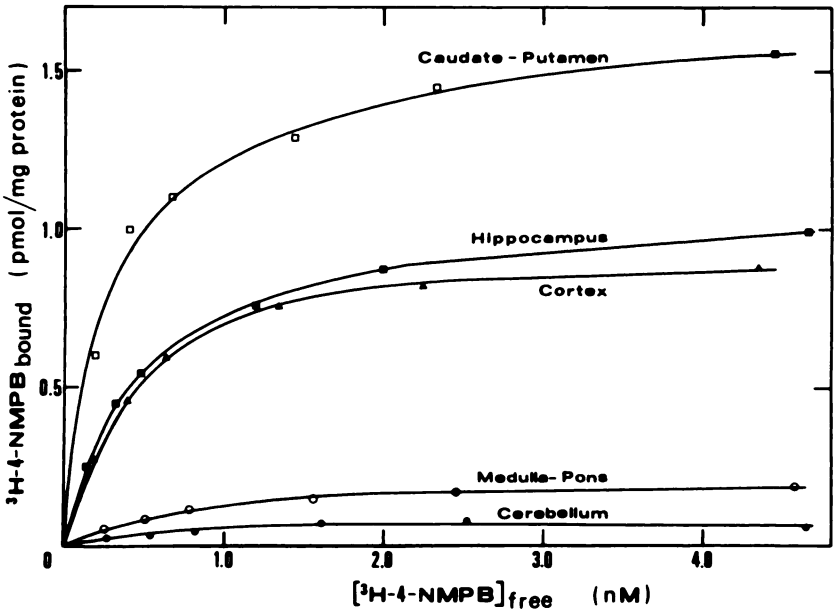

FIG. 1. *Specific binding of [^{3}H]-4NMPB at 25° as a function of ligand concentration*

0.05 ml tissue homogenate were incubated with varying concentrations of [^{3}H]-4NMPB for 30 min at 25° in 2 ml modified Krebs solution (pH 7.4). □—□ caudate putamen; ■—■ hippocampus; ▲—▲ cortex; ○—○ medulla; ●—● cerebellum. Each point is the mean of triplicate samples with standard error less than 5%.

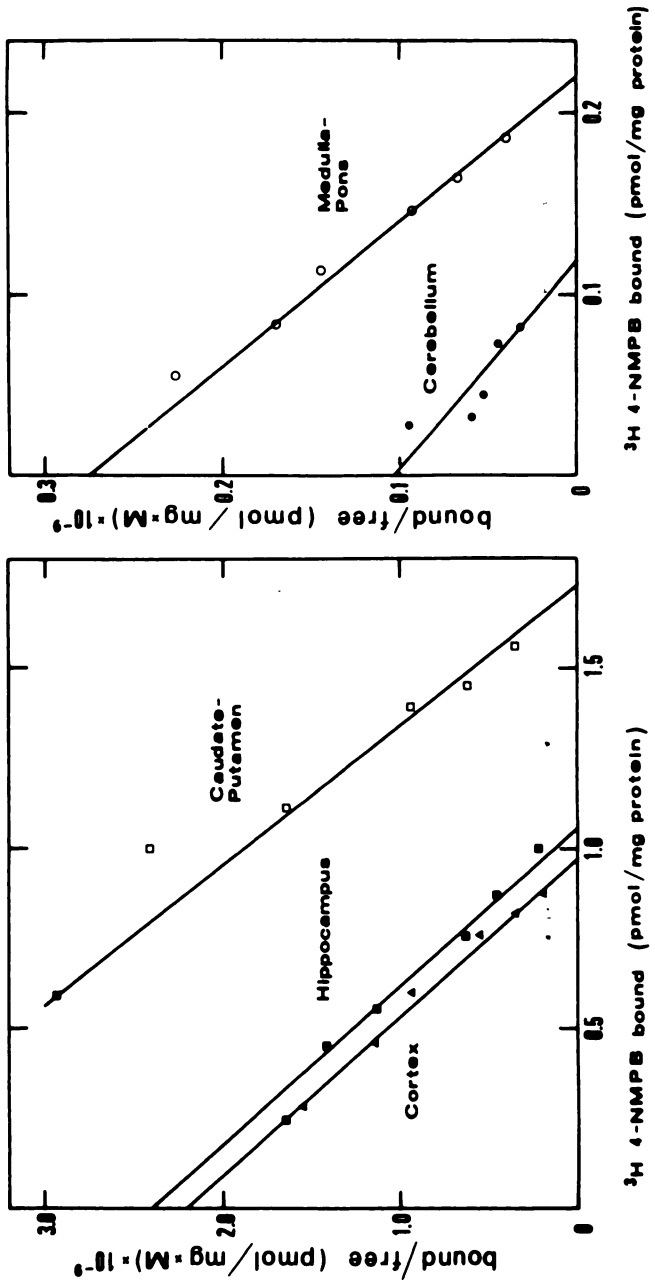

FIG. 2. *Scatchard plot of [³H]-4NMPB binding to homogenate of various brain regions at 25° (data of Fig. 1).*

TABLE 1

Regional distribution of specific [^{3}H]-4NMPB and [^{3}H]-atropine binding[a]

Region	K_D	[^{3}H]-4NMPB binding pmole/mg protein	K_D	[^{3}H]Atropine binding pmole/mg protein
	(nM)		(nM)	
Caduate putamen	0.38 ± 0.01	1.54 ± 0.38	1.02 ± 0.02	1.9 ± 0.38
Hippocampus	0.47 ± 0.03	1.05 ± 0.05		—
Cortex	0.41 ± 0.03	0.91 ± 0.06	1.5 ± 0.12	1.05 ± 0.12
Medulla pons	0.82 ± 0.02	0.26 ± 0.05	4.27 ± 0.32	0.31 ± 0.07
Cerebellum	1.15 ± 0.2	0.12 ± 0.01	—	—

[a] The values given are the mean of at least six separate binding curves ± SEM. K_D values are obtained from Scatchard plots. See text for description of binding assays.

to be slightly higher in the caudate putamen than in hippocampus and cortex, and there is a very marked difference between receptor density in these regions and the density in the cerebellum and medulla pons. The relative receptor-capacity in the latter regions compared to the first three is also reflected in the results obtained with [^{3}H]-atropine as the labeled ligand (Table 1).

The nature of the high affinity binding of [^{3}H]-4NMPB to the various preparations was tested by competition experiments in which selected unlabeled ligands with known muscarinic properties inhibit the binding of [^{3}H]-4NMPB. Figures 3 and 4 show the results of competition experiments in homogenates from hippocampus and medulla pons, respectively. The potent muscarinic antagonists (−) QNB, (+) QNB, scopolamine and atropine inhibit the binding of [^{3}H]-4NMPB in a competitive manner in all brain regions investigated.

The binding constants measured in these competition experiments are given in Table 2 and compared to the corresponding affinity constants in a pharmacological system. The K_D values in all brain regions investigated were found to be independent of receptor concentrations within the limits of accuracy of the assay. Note the excellent agreement between the K_D values measured for atropine from the competition experiment and from a direct binding assay with [^{3}H]-atropine. Equally significant for the characterization of the binding sites is the fact that the affinity ratio of the enantiomers as measured by the ratio of their K_D values, (−) QNB: (+) QNB (≃20), holds both for the binding experiments and for the bioassay in the intact organ (9, 13) (Table 2). The identical stereo-selectivity is a good indication that the structural integrity of the membrane preparation is preserved in the binding experiments.

The complex nature of the binding of agonists to the muscarinic receptor (14, 15) precludes a reliable determination of K_D values for agonists from competition experiments with [^{3}H]-4NMPB. An indication of the relative affinity of agonists for the binding sites labeled with [^{3}H]-4NMPB can nevertheless be obtained from the I_{50} values obtained for a series of muscarinic agonists. The concentration range at which sizable inhibition of [^{3}H]-4NMPB is obtained is 2–3 orders of magnitude higher than the concentrations at which these drugs act as muscarinic agonists.

The slopes of Hill plots obtained such as in Figs. 3 and 4 for both agonists and antagonists are given in Tables 2 and 3. The complex agonist binding properties of the muscarinic receptor were described previously by Birdsall and Hulme (14 and ref. therein), who suggested the presence of a heterogeneous population of agonist binding sites in rat cerebral cortex. In agreement with these observations (14) the slopes obtained here for the binding of muscarinic antagonists are not significantly different from 1.0, whereas the agonists exhibit lower values. This is observed in most brain regions studied here with some noteworthy exceptions such as the caudate putamen and hippocampus where the values for oxotremorine are also close to unity, as for

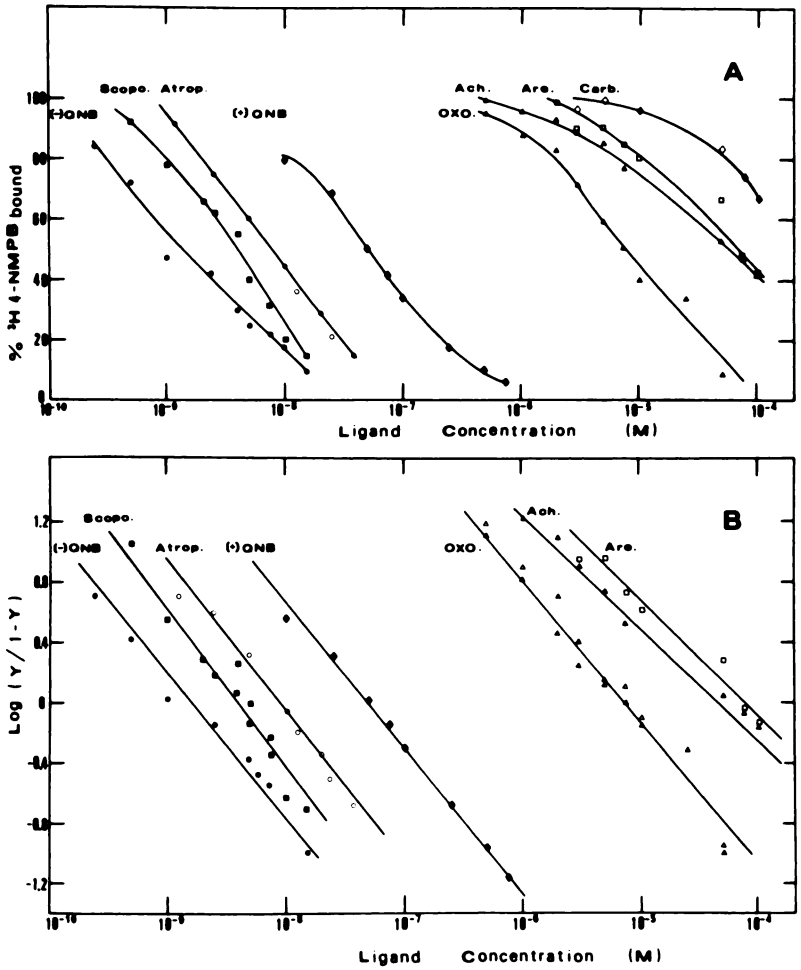

FIG. 3. *Competition binding of muscarinic drugs to hippocampus homogenates*

A. Samples (0.05 ml) were incubated at 25° for 30 min in 2 ml modified Krebs solution containing 2.0 nM [^{3}H]-4NMPB and the concentrations of unlabeled ligands indicated. Specific binding was determined as described in METHODS. Each point represents the average of two triplicate determinations. ●——●, (−)QNB; ■——■, scopolamine, ○——○ atropine; ◆——◆, (+)QNB; △——△, oxotremorine; ▲——▲, acetylcholine; □——□, arecoline and ◇——◇, carbamylcholine. B. Hill plot of the same data. Y is the fractional binding of [^{3}H]-4NMPB.

the antagonists. The reasons underlying such interesting exceptions are currently investigated.

Kinetics of the high-affinity binding. The time course of [^{3}H]-4NMPB binding at two ligand concentrations, corrected for non-specific binding, is presented in Fig. 5 for the medulla pons and in Fig. 6 for the caudate putamen. Binding appears to reach equilibrium within about 30 min of incubation with 0.5 nM ligand at 25°. In order to compare the association rates, conditions for the experiments were chosen for which the concentrations of receptor and labeled ligand were identical for the caudate putamen and the medulla pons (see legends to Figs. 5 and 6). As shown in these figures the half maximal binding occurs at 2.5 min in the medulla pons and at 7.8 min in the caudate putamen. Similarly, the rates of binding to the cortex and hippocampus preparations were slower than to the medulla pons while the value for the cerebellum was close to that of the medulla pons.

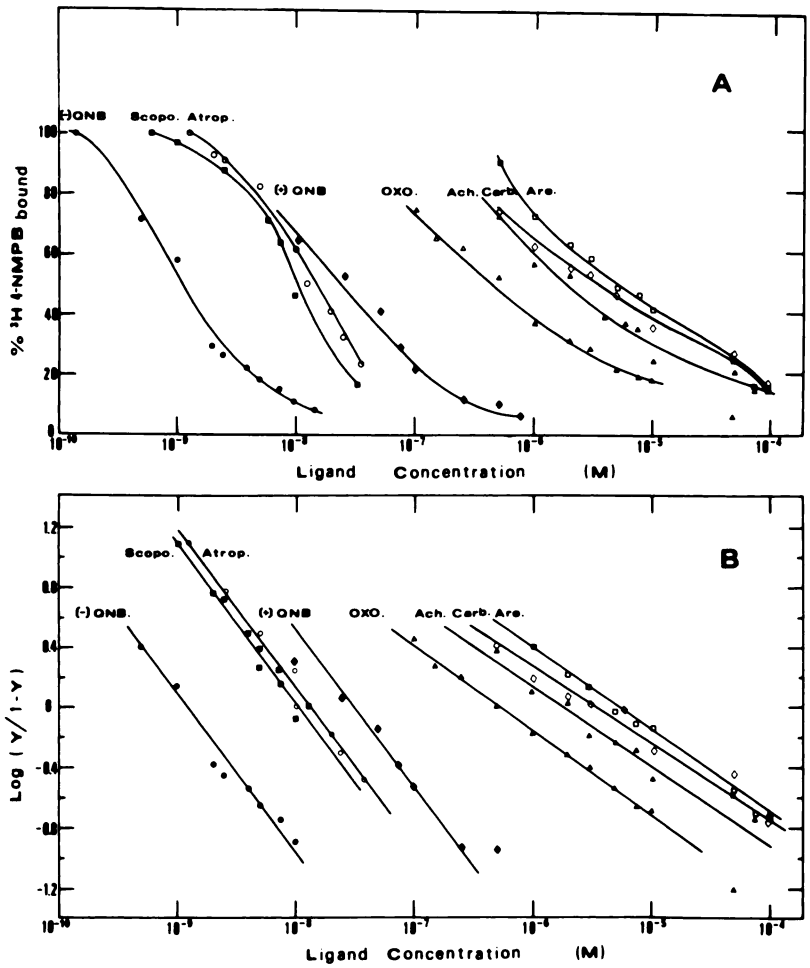

FIG. 4. *Competition binding of muscarinic drugs to the medulla pons homogenates*

A. Samples (0.05 ml) were incubated at 25° for 30 min in 2 ml modified Krebs solution containing 2.0 nM [^{3}H]-4NMPB and the concentration of unlabeled ligands indicated. Specific binding was determined as described in METHODS. Each point represents the average of two triplicate determinations. ●—● (−)QNB; ■—■, scopolamine, ○—○, atropine; ◆—◆, (+)QNB; △—△, oxotremorine; ▲—▲, acetylocholine; □—□, arecoline and ◇—◇, carbamlycholine. B. Hill plot of the same data. Y is the fractional binding of [^{3}H]-4NMPB.

The solid lines in Figs. 5 and 6 were obtained by curve fitting using a non-linear regression procedure for a simple bimolecular reaction scheme. By analogy to previous observations (2, 3) this overall behavior could in principle be attributed to a "true" simple bimolecular reaction, i.e., a single population of binding sites. Close inspection of the data shown in Figs. 5 and 6 suggests, however, a significant and systematic deviation. The systematic difference was that for short times the experimental points were higher (30%–40%) than the value expected from curve fitting; while for long times the deviation from the expected value was in the opposite direction (ca. 20%). This phenomenon was especially outstanding in experiments using low ligand concentrations and the tissues of cortex, hippocampus and caudate putamen. Such deviations are difficult to characterize from the relatively insensitive hyperbolic plots. To delineate the region where systematic deviations from simple single-population behavior of binding might occur, the data obtained were replotted in a linear form

TABLE 2

Binding constants (nM)[a] for muscarinic antagonists determined by direct[b] binding and competition with 2 nM [^{3}H]-4NMPB

Ligand	Pharmacological affinity constant[c]	Cortex	Caudate putamen	Hippocampus	Medulla pons	Cerebellum
[^{3}H]-4NMPB[b]	0.2	0.41 (1.02)[d]	0.38 (1.0)	0.47 (1.02)	0.82 (1.0)	1.15 (1.05)
(−)QNB	—	0.37 (1.1)	0.15 (0.98)	0.45 (0.96)	0.35 (0.95)	— —
Scopolamine	0.4	0.62 (0.97)	0.62 (1.1)	0.72 (1.05)	2.6 (1.0)	2.6 (1.07)
Atropine	0.5	1.1 (1.06)	0.91 (1.07)	1.4 (1.01)	4.0 (0.95)	4.1 (1.08)
[^{3}H]-Atropine[b]	—	1.5 (1.02)	1.02 (1.05)	— —	4.3 (0.99)	— —
(+)QNB	5	7.5 (0.99)	5.2 (0.95)	6.2 (0.95)	8.4 1.05	— —

[a] The average values of binding constants determined in 3 separate experiments each performed in triplicate whose results varied by less than 15%. Values for K_D for antagonists were calculated as described previously (1, 2), assuming a simple competitive interaction between 4-NMPB and the competing ligand. [^{3}H]-4NMPB binding sites concentrations (nM) were: cortex 0.14–0.22, caudate putamen 0.08–0.15, hippocampus 0.12–0.25, medulla pons 0.09–0.13, and cerebellum 0.06–0.09.

[b] Direct binding.

[c] These values refer to determinations of antimuscarinic potency in isolated guinea pig ileum. Data taken from references (35, 9, 13).

[d] Numbers in parentheses are Hill coefficients.

TABLE 3

I_{50} values (μM)[a] for muscarinic agonists determined by competition with 2 nM [^{3}H]-4NMPB

Ligand	Cortex	Caduate putamen	Hippocampus	Medulla pons	Cerebellum
Oxotremorine	4.8 (0.8)[b]	5.9 (1.0)	7.2 (0.95)	0.39 (0.5)	0.47 (0.4)
Carbamylcholine	170 (0.4)	>100 —	>100 —	4.7 (0.5)	5.5 (0.6)
Arecoline	55 (1.06)	40 (0.6)	72 (0.62)	4.2 (0.6)	— —
Acetylcholine	30 (0.6)	13 (0.5)	64 (0.7)	3.0 (0.5)	— —

[a] Values for K_D for agonists depend on their mode of binding and hence values of I_{50} are given, i.e., the concentration of drug causing 50% reduction in binding of [^{3}H]-4NMPB under the experimental conditions described. The average values of I_{50} determined in experiments similar to that in Figs. 3 and 4 are presented. Values given are the means of 3–4 separate experiments, each performed in triplicate, whose results varied by less than 15%. For cholinesterase-sensitive agonists the assay contained 10^{-5} M physostigmine. This concentration of inhibitor did not affect the binding characteristics of [^{3}H]-4NMPB in the absence of agonists. [^{3}H]-4NMPB binding site concentrations were as in Table 2.

[b] Numbers in parentheses are Hill coefficient.

using the integrated rate equation for bimolecular reaction:

$$\ln \frac{(B_{eq} - B_t)}{B_{eq}} = -(k_1[\text{4-NMPB}] + k_{-1}) \cdot t \quad (1)$$

where B_{eq} and B_t are the concentrations of bound receptor at equilibrium and at time t. Free 4-NMPB is in great excess and therefore can be considered constant throughout the reaction. Under such pseudo first order conditions, data plotted according to Eq. 1 should yield straight lines if the reaction is bimolecular.

The actual results obtained from a plot of this equation for different concentrations of [^{3}H]-4NMPB are shown in Fig. 7 for medulla pons and caudate putamen. The plots are linear only at high concentrations of labeled ligand. Similar biphasic behavior was observed for the binding of [^{3}H]-4NMPB to homogenates from the other regions studied: cortex, cerebellum and hippocampus. The dependence of the fraction of receptors reaching in the first phases of reactions on ligand concentration (Fig. 7) is inconsistent with the assumption of two independent classes of sites and is consistent with an isomerization step of ligand-receptor complex (vide infra).

To complete the dynamic picture of

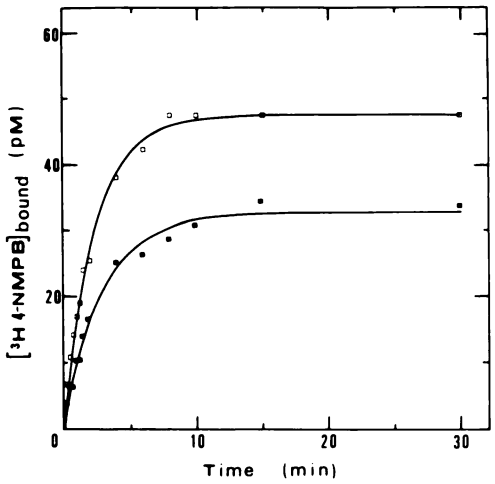

FIG. 5. *Time course of association of [^{3}H]-4NMPB to medulla pons preparation at 25°*

Samples (0.05 ml) were incubated in 2 ml modified Krebs solution with ligand for various periods of time. Specific binding was determined as described in METHODS. Receptor binding sites concentration was 66 pM. Each experimental point is the mean of triplicate samples whose standard error was less than 5%. The kinetics were measured with [^{3}H]-4NMPB at the following concentrations: ■—■, 0.5 nM; □—□, 1.0 nM.

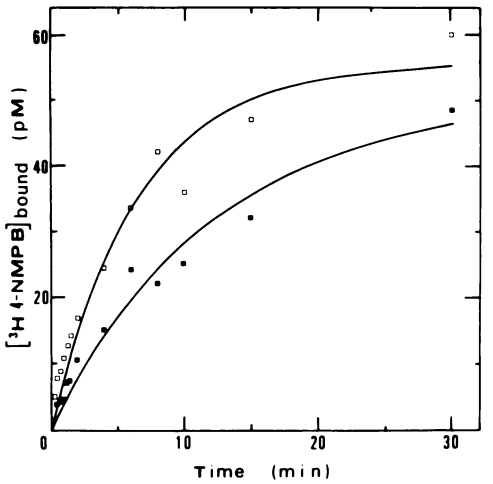

FIG. 6. *Time course of association of [^{3}H]-4NMPB binding to homogenate of caudate putamen*

For details see legend to Fig. 5. Ligand concentrations: ■—■, 0.5 nM, □—□ 1 nM; receptor binding sites concentration 62 pM.

[^{3}H]-4NMPB binding, the rate of dissociation of the ligand from each of the separate brain regions was determined by the technique of isotopic dilution (see legend to Fig. 9 for details). The first order plots for the dissociation of [^{3}H]-4NMPB from the various preparations shown in Fig. 8 deviate from linearity, indicating again that more than one kind of ligand-receptor complexes may exist in the various regions of mouse brain preparations. This phenomenon was observed previously with whole mouse brain preparation (2, 3). The dissociation data can be fitted with the sum of at least two first order exponential terms. For example, the dissociation has been fitted here to the equation:

$$Y = \alpha_1 e^{-k_{-1}t} + \alpha_2 e^{-k_{-2}t}$$

where k_{-1} and k_{-2} are the first order rate constants corresponding to the fractions α_1 and α_2 of binding sites.

The parameters of this fit (i.e., rate constants and coefficients) as well as calculated half-life times for the dissociation, are given in Table 4. As shown, the $t_{1/2}$ for the dissociation from the cortex is 20 min while that from the medulla pons is 5 min. Again, as in the case of the binding experiments this strongly suggests heterogeneity.

DISCUSSION

Regional distribution and characteristics of muscarinic high-affinity binding sites. The binding of [^{3}H]-atropine and [^{3}H]-4NMPB to various regions of mouse brain homogenates bears the characteristics of specific interactions with muscarinic acetylcholine receptors: i) saturability (Fig. 1) at very low concentrations (i.e., high affinity); ii) similar binding capacity (Table 1) for different labeled muscarinic antagonists; iii) direct relation to the muscarinic profile and rank order of potency of both agonists and antagonists (Tables 2 and 3), including specific muscarinic stereoselectivity (e.g., the potency ratio of QNB enantiomers—Table 2). The very low levels of non-specific binding allowed us to obtain reliable equilibrium binding data in several separate regions of the mouse brain in spite of the relatively small number of receptors in some of these regions (Table 1). In agreement with neurophysiological data (16, 17), we found marked variations in the maximal

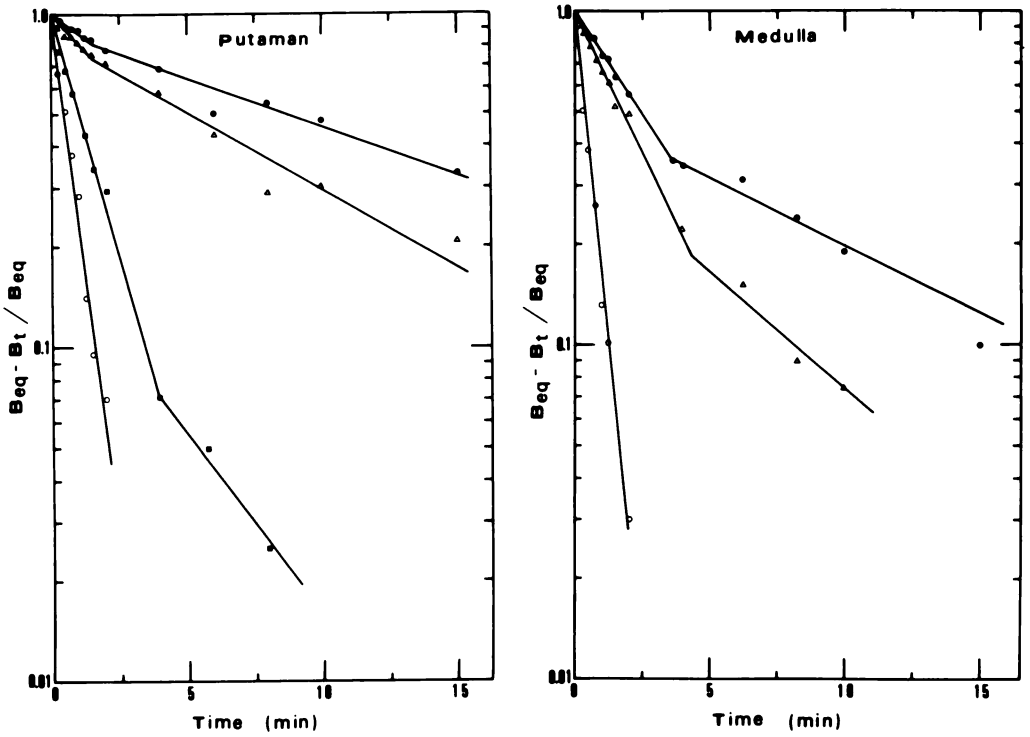

FIG. 7. *Initial rate of [^{3}H]-4NMPB binding at different ligand concentrations to caudate putamen (left) and medulla (right) preparations*

Homogenates were incubated with 0.5 nM (●), 1.0 nM (△), 2.0 nM (■) and 5.0 nM (○) [^{3}H]-4NMPB at 25° for the various time intervals. Association was begun by addition of tissue (62 pM and 66 pM binding sites for the putamen and medulla, respectively), and terminated by rapid filtration, as described in METHODS. The data are plotted according to the equation described in the text. The data presented are from a single experiment performed in triplicate (standard error was less than 5%), which was replicated twice.

number of high affinity binding sites that bind [^{3}H]-4NMPB: caudate putamen, hippocampus and cortex had the highest concentration of binding sites, while the medulla pons and the cerebellum showed the lowest binding capacity per mg protein (Table 1). This distribution is in agreement with known distributions of muscarinic receptors in other mammalian brains, and it parallels the distribution of acetylcholine and its synthetic and degradative enzymes in these systems (8, 18–20).

The equilibrium binding studies in homogenates from the separate regions presented here indicate an interaction of the labeled ligand with a homogeneous population of binding sites within each preparation (e.g., Fig. 2). Data in Table 2, however, clearly demonstrate some small but consistently reproducible differences between the K_D values of [^{3}H]-4NMPB on the high affinity binding sites in various regions of mouse brain. Thus, while the K_D values in the cortex, caudate putamen and the hippocampus are very similar, the muscarinic ligand seems to have a consistently lower affinity for the binding sites in the cerebellum and medulla pons. This trend is reproduced with the other labeled antagonists: [^{3}H]-atropine and the unlabeled drugs for which the dissociation constants were measured by competition. Notably, the K_D values in pharmacological preparations resemble more the high affinity characteristics of the cortex, caudate putamen and hippocampus than the lower affinity of the medulla and cerebellum (Table 2).

It is also noteworthy that the degree of heterogeneity, as measured by differences in K_D values for the various regions, seems

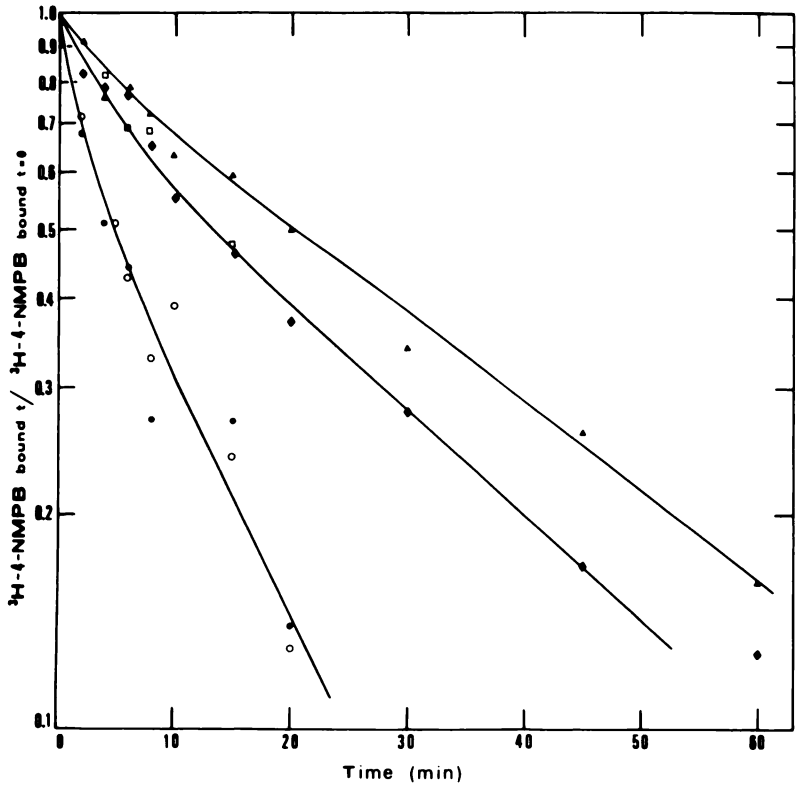

FIG. 8. *Dissociation of [^{3}H]-4NMPB from the muscarinic receptors in the various tissue preparations*

Samples (0.05 ml) were incubated to equilibrium at 25° in the presence of 5 nM [^{3}H]-4NMPB. Dissociation was begun by addition of 50 μM 4-NMPB to tubes and the samples were filtered immediately (zero time) and at the times indicated. Specific binding was determined as described in the text. Each point is the mean of at least three experiments whose standard error was less than 5%. ([^{3}H]-4NMPB$_{bound})_{t=0}$ was 0.87 pmole/mg protein for the cortex (▲), 1.0 pmole/mg protein for the hippocampus (◆), 1.45 pmole/mg protein for the caudate putamen (□), 0.29 pmole/mg protein for the medulla pons (○), and 0.11 pmole/mg protein for the cerebellum (●).

TABLE 4

Kinetic parameters for binding of [^{3}H]-4NMPB to various brain regions

Region	Association experiments	Dissociation experiments[b]				
	$K_{on} \times 10^8$ (M^{-1} min^{-1})[a]	k_{-1} (min^{-1})	k_{-2} (min^{-1})	α_1	α_2	$t_{1/2}$
Cortex	2.45	0.028	0.44	0.88	0.12	20
Caduate putamen	2.57	0.05	—	0.92	0.08	16
Hippocampus	2.28	0.021	0.09	0.45	0.55	16
Medulla pons	4.03	0.05	0.21	0.21	0.79	5
Cerebellum	5.83	0.036	0.3	0.35	0.65	5

[a] Values calculated from initial rates.

[b] Calculated according to equation $Y = \alpha_1 e^{-k_{-1}t} + \alpha_2 e^{-k_{-2}t}$ as described previously (2). Data calculated from at least three separate experiments performed in triplicate (see legend to Fig. 8).

to depend somewhat on the nature of the ligand. Thus, the K_D values measured in cortex, caudate putamen and hippocampus differ less from K_D values in medulla pons and cerebellum if the ligand used is a benzilate derivative (e.g., 4-NMPB, QNB) than if the ligand is a tropate (i.e., atropine, scopolamine). It is difficult to conclude at

this stage whether this finding is directly related to differences in the large variety of pharmacological effects exhibited by these structural classes of drugs, and whether the differences observed between them constitute a significant element in their modes of action.

In contrast to this trend in the affinity of antagonists for the binding sites in the various brain regions, the competition experiments with muscarinic agonists revealed an opposite and even more pronounced regional difference: the affinity of agonists (measured as I_{50}) for the sites in the cerebellum and medulla pons can be more than one order of magnitude higher than the affinity for the binding sites in mouse cortex, caudate putamen or hippocampus (Table 3). This consistency in the regional grouping of muscarinic binding sites by a criterion of affinity (albeit with opposite trends for agonists and antagonists) provides a very strong indication that the observed differences in K_D reflect a regional heterogeneity of muscarinic receptors in mouse brain. This suggestion was further investigated, and received additional support, from the kinetic analysis of [^{3}H]-4NMPB binding in the various regions.

Kinetics of association and dissociation of [^{3}H]-4NMPB from muscarinic binding sites. As shown from the equilibrium binding experiments, the data from the kinetics of association and dissociation of [^{3}H]-4NMPB also suggest that the five brain regions studied may be grouped into two subsets containing binding sites of slightly different character. Thus, Table 4 shows that the association constants (k_{on}) in the cerebellum and medulla pons are different from the constants measured for the other group composed of the cortex, hippocampus, and the caudate putamen. The same grouping is also apparent in the results from the dissociation experiments (Table 4): the apparent half-life times ($t_{1/2}$) of the dissociation of [^{3}H]-4NMPB from binding sites in the cerebellum and medulla pons are three to four times shorter than for the dissociation from the other three regions. It appears therefore that the trend in the kinetics of association and dissociation of [^{3}H]-4NMPB from muscarinic binding sites in the various regions of mouse brain is entirely consistent with the reproducible differences in K_D measured for the ligand in the same regions. These findings lend additional support to our conclusion that within the set of conditions created by our standard methods for the definition and characterization of receptors by labeled ligands, mouse brain homogenates exhibit regional heterogeneity of high affinity muscarinic binding sites.

The simplest mechanism that would explain the biphasic behavior observed here for [^{3}H]-4NMPB association to the muscarinic binding sites in each of the studied brain regions were summarized recently by Galper *et al.* (4) and Sugiyama *et al.* (5). Our results (Figs. 7 and 8) are equally inconsistent with a simple bimolecular mechanism. Moreover, the dependence of the fraction of receptors reacting in the first phases of reaction on ligand concentration (Fig. 7) and the deviation of the dissociation kinetics from first order behavior (Fig. 8, Table 4) strongly suggest an isomerization of the ligand-receptor complex. Such a mechanism was proposed earlier by us from kinetic data on the interaction of [^{3}H]-4NMPB with muscarinic binding sites in whole mouse brain homogenates (1–3). Data suggesting an isomerization step of the ligand (L)-receptor(R) complex (LR) to a different form (LR*):

$$L + R \rightleftarrows LR \rightleftarrows LR^*$$

has now been reported independently for chick heart (4) and retina (5). Recent characterizations of muscarinic receptors in the irides of rabbit (6), and cat (7) yielded similar results, thus increasing the variety of systems and animal species in which an isomerization step appears to be related to the interaction of antagonists with muscarinic receptors. The receptor population within each one of the mouse brain regions studied here appears however to be homogeneous, as seen also from the equilibrium binding experiments described above.

According to a previous report (2), binding studies to whole mouse brain homogenate indicated that [^{3}H]-4NMPB or [^{3}H]-scopolamine binding could not be fitted and analyzed in terms of a simple population of

binding sites. The Scatchard plots for the binding of the two ligands deviated from linearity, in contrast to the binding of [^{3}H]-atropine which gave straight lines. This could be explained as a combination of at least two complementary factors: (a) differences in the values of K_D for the receptor of each region in the brain, (b) differences in the specific densities of receptors located in different regions. It is important to note that the regions investigated here represent no more than 55% of the whole brain.

The functional role of the isomerization step may be related to the models that have been invoked to explain receptor interactions of both agonists and antagonists with nicotinic (21–29) and muscarinic receptors (14, 29–33). Recent work on agonist-induced desensitization phenomena (see, for example, Grunhagen and Changeux (23) and ref. therein) is of particular interest in the context of the present work. The antagonist-induced generation of more than one receptor conformer might well be analogous to those structural changes which find their physiological expression in the form of desensitization; this most probably indicates a common feature pertaining to all ligand-receptor complexes with agonists as well as antagonists.

The dramatic changes in the I_{50} profile of the various agonists when considered together with the kinetics of binding are consistent with the hypothesis of functional heterogeneity of the muscarinic receptor in the mouse brain. It is noteworthy that receptor heterogeneity was also implicated in the interaction of muscarinic receptors with weak antagonists (34).

ACKNOWLEDGMENTS

Enlightening discussions on this subject with N. Zisapel, H. Weinstein and D. Michaelson, are gratefully acknowledged. Mrs. Ronit Galron provided excellent technical assistance.

REFERENCES

1. Kloog, Y. & Sokolovsky, M. (1977) Muscarinic acetylcholine interactions: Competition binding studies with agonists and antagonists. *Brain Res.* **134,** 167–172.
2. Kloog, Y. & Sokolovsky, M. (1978) Studies on muscarinic acetylcholine receptors from mouse brain: Characterization of the interaction with antagonists. *Brain Res.* **144,** 31–48.
3. Kloog, Y. & Sokolovsky, M. (1978) Muscarinic binding to mouse brain receptor sites. *Biochem. Biophys. Res. Commun.* **81,** 710–717.
4. Galper, J. B., Klein, W. & Catterall, W. A. (1977) Muscarinic acetylcholine receptors in developing chick heart. *Biol. Chem.* **252:** 8692–8699.
5. Sugiyama, H., Daniels, M. P. & Nirenberg, M. (1977) Muscarinic acetylcholine receptors of developing retina. *Proc. Natl. Acad. Sci. U.S.A.* **74,** 5524–5528.
6. Kloog, Y., Heron, D. S., Korczyn, A. D., Sachs, D. I. & Sokolovsky, M. (1979) Muscarinic acetylcholine receptors in albino rabbit iris-ciliary body. *Mol. Pharmacol.* **15,** in press.
7. Kloog, Y., Sachs, D. I., Korczyn, A. D., Heron, D. S. & Sokolovsky, M. Muscarinic acetylcholine receptors in cat iris. *Biochem. Pharm.* in press.
8. Kloog, Y., Egozi, Y. & Sokolovsky, M. (1979) Regional heterogeneity of muscarinic receptors of mouse brain. *FEBS Lett.* **97,** 265–269.
9. Rehavi, M., Maayani, S. & Sokolovsky, M. (1977) Enzymatic resolution and cholinergic properties of (±)3-Quinuclidinol derivatives. *Life Sci.* **21,** 1293–1302.
10. Slotnick, B. M. & Leonard, C. M. (1975). In *A Stereotaxic Atlas of the Albino Mouse Forebrain,* DHEN publication, U.S. Government Printing Office, Wash., D.C.
11. Lowry, O. H., Rosebrough, N. J., Farr, A. L. & Randall, R. J. (1951) Protein measurement with the folin reagent. *J. Biol. Chem.* **193,** 265–275.
12. Scatchard, G. (1949) The attraction of proteins for small molecules and ions. *Ann. N.Y. Acad. Sci.* **51,** 660–672.
13. Rehavi, M., Yaavetz, B., Kloog, Y., Maayani, S. & Sokolovsky, M. (1978) In vivo and in vitro studies on the antimuscarinic activity of some amino esters of benzilic acid. *Bioch. Pharm.* **27,** 1117–1124.
14. Birdsall, N. J. M. & Hulme, E. C. (1976) Biochemical studies on muscarinic acetylcholine receptors. *J. Neurochem.* **27,** 7–16.
15. Taylor, I. K., Cuthbert, A. W. & Young, J. M. (1975) Muscarinic receptors in rat intestinal muscle: Comparison with the guinea pig. *Eur. J. Pharmacol.* **31,** 319–326.
16. Krnjevic, K. & Phillis, J. W. (1963) Acetylcholine-sensitive cells in the cerebral cortex. *J. Physiol. London* **166,** 296–328.
17. McLennan, H. & York, D. H. (1966) Cholinergic mechanisms in the caudate nucleus. *J. Physiol. London* **187,** 163–172.
18. Hiley, C. R. & Burgen, A. S. V. (1974) The distribution of muscarinic receptor sites in the nervous system of the dog. *J. Neurochem.* **22,** 159–162.

19. Snyder, S. H., Chang, K. J., Kuhar, M. J. & Yamamura, H. I. (1975) Biochemical identification of the mammalian muscarinic cholinergic receptor. *Fed. Proc.* **34,** 1915–1921.
20. Yamamura, H. I., Wastek, G. J., Johnson, P. C. & Stern, L. A. (1978) In *Cholinergic Mechanisms and Psychopharmacology,* D. J. Jenden, ed., Plenum, New York, 35–49.
21. Barrantes, F. J. (1976) Intrinsic fluorescence of the membrane bound acetylcholine receptor: Its quenching by suberylcholine. *Biochem. Biophys. Res. Comm.* **72,** 479–488.
22. Bonner, R., Barrantes, F. J. & Jovin, T. M. (1976) Kinetics of agonist-induced intrinsic fluorescence changes in membrane-bound acetylcholine receptor. *Nature (Lond.)* **263,** 429–431.
23. Grunhagen, H. H. & Changeux, J. P. (1976) Studies on the electrogenic action of acetylcholine with torpedo marmorata electric organ. V. Qualitative correlation between pharmacological effects and equilibrium processes of the cholinergic receptor protein revealed by the structural probe quinacrine. *J. Molec. Biol.* **106,** 517–535.
24. Karlin, A. (1967) On the application of "a plausible model" of allosteric proteins to the receptor for acetylcholine. *J. Theoret. Biol.* **16,** 306–320.
25. Maelicke, A. & Reich, E. (1976) In *The Structural Basis of Membrane Function,* Y. Hatefi and L. Djavadi-Ohaniance, eds., Academic Press, New York, 363–374.
26. Neuman, E. & Van Change, Hai (1976) Dynamic properties of isolated acetylcholine receptor protein: Kinetics of the binding of acetylcholine and Ca ions. *Proc. Natl. Acad. Sci. U.S.A.* **73,** 3994–3998.
27. Raftery, M. A., Vandlen, R. L., Reed, K. L. & Lee, T. (1976) Characterization of *Torpedo Californica* acetylcholine receptor: Its subunit composition and ligand-binding properties. *Cold Spr. Harb. Symp. Quant. Biol.* XL, 193–202.
28. Rang, H. P. & Ritter, J. M. (1969) A new kind of drug antagonism. Evidence that agonists cause a molecular change in acetylcholine receptors. *Mol. Pharmacol.* **5,** 394–411.
29. Rang, H. P. & Ritter, J. M. (1970) The relationship between desensitization and the metaphilic effect at cholinergic receptors. *Mol. Pharmacol.* **6,** 383–390.
30. Ariens, E. J. & Simonis, A. M. (1967) Cholinergic and anticholinergic drugs, do they act on common receptors? *Ann. N.Y. Acad. Sci.* **144,** 842–868.
31. Barlow, R. B., Lowe, B. M., Pearson, J. D. M. Randall, H. M. & Thompson, G. M. (1971) Ion size and activity at acetylcholine receptors. *Mol. Pharmacol.* **7,** 357–366.
32. Gupta, S. K., Moran, J. F. & Triggle, D. J. (1976) Mechanism of action of benzilylcholine mustard at the muscarinic receptors. *Mol. Pharmacol.* **12,** 1019–1026.
33. Snyder, S. H. (1975) Neurotransmitter and drug receptors in the brain. *Biochem. Pharmacol.* **24,** 1371–1374.
34. Fisher, A., Grunfeld, Y., Weinstock, M. Gitter, S. & Cohen, S. (1976) A study of muscarinic receptor heterogeneity with weak antagonists. *Eur. J. Pharmacol.* **38,** 131–139.
35. Paton, W. D. M. (1961) A theory of drug action based on the rate. *Proc. Roy. Soc. B.* **154,** 21–69.